

# Hydrodynamics and rheology of a dilute granular plane Couette flow

Ronak Gupta<sup>1,\*</sup> and Meheboob Alam<sup>2</sup>

<sup>1</sup>Matière et Systèmes Complexes - CNRS, University of Paris Cite, Paris, France

<sup>2</sup>Jawaharlal Nehru Centre for Advanced Scientific Research, Jakkur PO, Bengaluru 560064, India

**Abstract.** We simulate the plane Couette flow of a dilute granular gas using the Direct Simulation Monte Carlo method. We calculate relevant hydrodynamic and rheological quantities and highlight the effects of driving shear rate and inelasticity on them. Our results reveal the competing effects of dissipation-induced particle clustering and shear-induced de-clustering on hydrodynamic and rheological fields and call for suitable modifications in theoretical models that predict the flow of rarefied granular gases.

## 1 Introduction

In the past few decades, advances have been made in studying a system of suspended particles usually driven by a source of energy and interacting only via binary inelastic collisions. Under strong driving (say, via shaking or shear), the particles fly around randomly with large inter-particle separation, analogous to a dilute molecular gas: such a dilute system of macroscopic particles is dubbed a *granular gas* [1–3]. Prototypical flows of granular gases have been studied by various researchers using a combination of theoretical, experimental and computational approaches [1–8]. Granular gas dynamics are interesting and challenging because of important feature in which granular gases differs from the traditional molecular gas: the constituent particles in a granular gas suffer *inelastic* collisions and hence loose energy via collisions. The latter is responsible spontaneous clustering of particles (density inhomogeneity) as well as a lack of scale separation [3]. The goal of this paper is to ascertain the roles of imposed shear and the particle inelasticity on hydrodynamic and rheological quantities in a simple canonical flow - the plane Couette flow of a dilute granular gas.

## 2 Methods

We simulate a granular plane Couette flow using the Direct Simulation Monte Carlo (DSMC) method - a stochastic particle-based technique, originally developed to simulate flows of rarefied molecular gases [9, 10]. DSMC differs from the deterministic Molecular Dynamics (MD) method in as it integrates the inelastic Boltzmann Equation rather than the Newton’s equations of motion for individual particles. Thus, the ‘particles’ in DSMC are basically quasi-particles that are used to increment the probability distribution and thus only have statistical significance and no physical meaning. DSMC ensures that, on average, the correct number of binary collisions are processed as mandated by kinetic theory. For a large number of simulated particles, one can then calculate moments of the distribution function and obtain relevant hydrodynamic and density flux.

### 2.1 Simulation details

To simulate a granular Couette flow, we have spherical inelastic particles, modelled as hard spheres bound by two

\*e-mail: ronakguptaa4186@gmail.com

walls separated by a distance  $L_y$  that move in opposite directions with speeds  $U^+$  and  $U^-$  (see figure 1). This breaks symmetry in the transverse direction,  $y$  and leads to a steady state 1-D flow in which all physical quantities are functions of  $y$  only. Our simulation domain is thus divided into  $N_{cells}$  cells with unit dimension in  $x$  and  $z$  directions and having thickness  $\delta y$  such that  $L_y = N_{cells}\delta y$ . The implementation of boundary conditions in DSMC is similar to MD since the simulation particles are treated as physical particles for the application of boundary conditions. Our simulation domain is *periodic* in  $x$  and  $z$  directions and for  $y$  directions we model the walls as *thermal* walls that are fully diffuse and have a temperature  $T_w$ . Details of boundary condition implementation is outlined in our previous work [11].

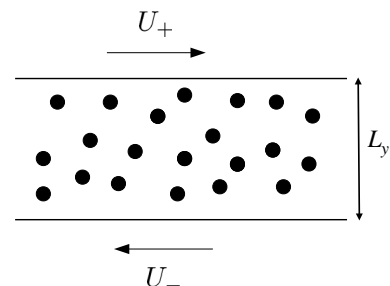


**Figure 1.** Setup for a plane Couette flow of a gas enclosed by two boundaries moving with speeds in opposite directions.

### 2.2 Control parameters

To simulate a dilute granular gas, we fix the average number density,  $n_{avg} = 0.00242$  (note that particle diameter,  $d = 1$ ). If we choose  $L_y$  to be the same for all simulations, it fixes the global Knudsen number,  $Kn = \lambda/L_y$  where  $\lambda$  is the equilibrium mean free path. We choose  $L_y$  such that  $Kn = 0.05$  for all simulations. As DSMC requires that  $\delta y$  should be a fraction of  $\lambda$  at all times, fixing the  $Kn$  also sets a bound for appropriate value of  $\delta y/N_{cells}$  which we obey. There are now two main control parameters in our system : (i) the normal restitution coefficient  $e_n$ , (ii) the dimensional shear rate  $\gamma$  :

$$\gamma = \frac{U_+ - U_-}{L_y} = \frac{\Delta U}{L_y} \quad (1)$$

In simulations we vary the shear rate by changing the magnitude of  $U$ , keeping the width,  $L_y$  fixed. Wall velocity

is given in units of the most probable velocity ( $u_{mpv} = \sqrt{2k_B T_w/m}$ ) and all values of shear rate reported are scaled by  $\gamma_c = \sqrt{2k_B T_w/m}/\lambda$ . We fix,  $m, d, k_b, T_w$  as 1 and choose  $n_{avg}, T_w, u_{mpv}, L_y$  to nondimensionalize  $n, T, u, y$ , respectively.

### 2.3 Code Validation

Here we reproduce the simulation results from a previous work on the Couette-Fourier flow of a dilute granular gas [12]. Note that in this work, the present Couette flow exists as a special case in which  $\Delta T_w = T_w^+ - T_w^- = 0$ , where +/- refer to upper and lower walls, respectively. In figure 2 we plot the variation of the bulk-averaged reduced shear viscosity,  $\eta^*$  with reduced shear-rate  $a$  as defined below:

$$\eta^* = \left\langle p_{xy}/\eta_0 \frac{du_x}{dy} \right\rangle \quad \text{and} \quad a = \left\langle \frac{1}{v_0} \frac{du_x}{dy} \right\rangle. \quad (2)$$

Here,  $\eta_0$  as the shear viscosity for elastic gases [13, 14] and  $v_0$  as the collision frequency [12].

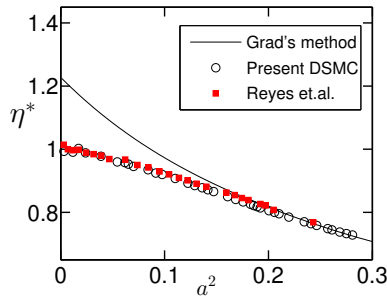


**Figure 2.**  $\eta^*$  vs  $a^2$  (Eq. 2) for  $T_w^+/T_w^- = 10$  and  $e_n = 0.9$ . Grad solution and red squares are taken from Reyes et.al [12].

It is evident from figure. 2, our DSMC code is able to accurately reproduce the results of simulating an inhomogeneous system very similar to what we undertake in the current work. For more validation checks the reader is referred to our previous works [15, 16]. It should be noted that the present simulations complement the work of Reyes *et al.*[12] that focussed largely on hydrodynamic fields in Couette-Fourier flow with  $\Delta T_w \neq 0$ .

### 3 Results and discussion

We first present number density profiles for two representative shear rates and three different values of  $e_n$  in figure 3. For the lower shear rate, the dissipation-induced clustering is responsible for the density peaks seen for  $e_n = 0.9$  and  $0.7$  whereas the density profile for  $e_n = 0.99$  shows a minima at the channel centre. The centreline peak for density disappears for all the shown values of  $e_n$  for the higher value of shear rate in figure 3(b) indicating that there is some rarefaction phenomena taking place on increasing shear rate. It must be noted that for all simulations, the global value of  $Kn$  is fixed to 0.05, a value where rarefaction effects are not expected to be very effective.

However, if we locally scale the shear rate by collision frequency  $v_0$ , the dimensionless local shear rate  $a$  (same

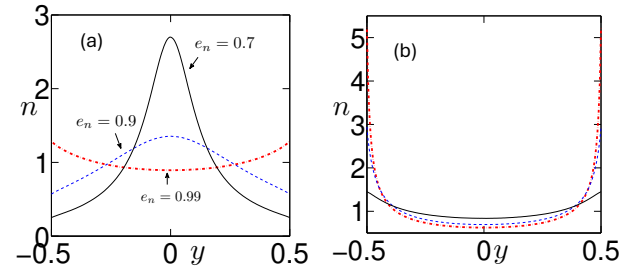


**Figure 3.** Number density profiles across channel width at (a)  $\gamma = 80$  and (b)  $\gamma = 400$  for  $e_n = 0.7, 0.9$  and  $0.99$ .

as the reduced shear rate,  $a$  within the brackets in Eq. 2), takes the form of a local Knudsen number  $Kn$  with hydrodynamic length scale  $h$ , given by  $v_T(\partial u_x/\partial y)^{-1}$  with  $v_T$  being the thermal velocity and  $\lambda = v_0/v_T$  [17]. The increase in global applied shear rate can be thus physically interpreted to an increase in  $Kn$ , inducing rarefaction effects. There must exist a critical value of the applied shear rate across which the centreline density curvature has a change in sign - a signature of rarefaction induced declustering. We show a phase plot in the  $(\gamma, 1 - e_n)$ -plane in Fig 4(a) where the solid line represents the boundary at which the centreline density curvature is zero.

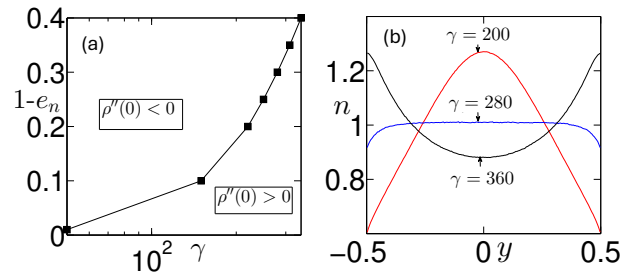


**Figure 4.** (a): Phase plot showing regions of positive and negative  $\rho''(0)$ , (b):  $n$  vs  $y$  for  $e_n = 0.7$  for different  $\gamma$ .

Clearly, for a lower value of  $e_n$ , a higher value of  $\gamma$  is required to prevent dissipation induced clustering. The 'switch' between signs of  $\rho''(0)$  is responsible for some features in other hydrodynamic fields and rheology. To elucidate this transition, figure 4(b) shows the density field for  $e_n = 0.7$  and three different values of  $\gamma$ , one each from the two regions of the phase-map and one on the phase boundary ( $\gamma \approx 280$ ) in figure 4(a). The sign change of  $\rho''(0)$  from negative to positive on increasing  $\gamma$  is evident in figure 4(b). Temperature profiles are inverse of density profiles,  $T \sim n^{-1}$ , that follows from the equation of state for constant pressure ( $p = nT$ ). Thus, when the curvature of density is positive at the centreline, the temperature curvature  $T''(0)$  is oppositely signed. For small  $\gamma$ , inelastic collisional 'cooling' is more effective, whereas at large  $\gamma$  the viscous heating leads to higher temperatures with a greater tendency of temperature profiles with a positive curvature as seen in figure 5(b). Strictly speaking, at any value of  $\gamma$ , the value of  $e_n$  determines the balance between 'cooling' and heating and hence the temperature profile

curvature and strength of the gradients as seen in figure 5(a). Essentially a phase plot similar to figure 4(a) can be constructed for temperature curvature as well. It will simply be complementary to figure 4(a) in the absence of temperature bimodality. The centreline curvature of temperature changes sign across the same phase boundary as density. This phase boundary also controls (1) : region of validity of the theoretical solution for the Couette flow of a heated granular gas [17] and (2) : region where the predictions of Grad's solution for the Couette flow of a granular gas become worse when compared to DSMC [12]. One of the core goals of this paper is to highlight how this phase boundary also mediates the behaviour of higher order rheological quantities.

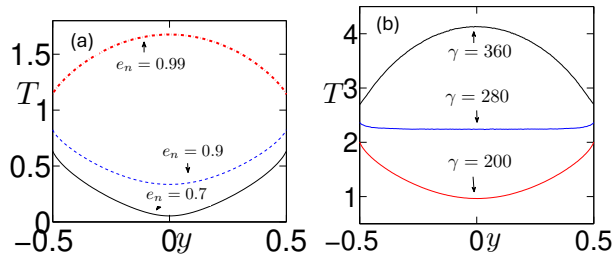


**Figure 5.** Temperature profiles for (a) different  $e_n$  at  $\gamma = 80$  and (b) different  $\gamma$  at  $e_n = 0.7$ .

We move on to results for higher order fields - in the absence of a body force in  $y$  direction, the pressure  $p$  remains constant across the channel. This is observed in our simulations as well, except near the walls. We see the same trend for shear-stress,  $p_{xy}$ . Calculating the reduced viscosity,  $\eta$  the same way as  $\eta^*$  in equation 2 reveals that  $\eta$  is a strong function of  $e_n$  and increases with increasing  $e_n$ . This holds for the values of  $\gamma$  (except at the lowest end), at least in a bulk-averaged sense, as seen in figure 6. This trend also agrees with theoretical predictions [18] and event-driven simulations [19] for the uniform shear flow of a dilute granular gas.

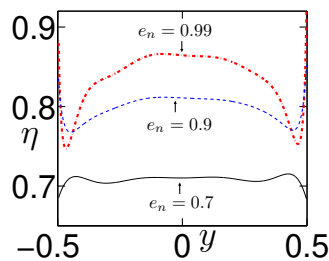


**Figure 6.** Shear viscosity profiles across channel width for  $e_n = 0.7, 0.9, 0.99$  with  $\gamma = 400$ .

We now move our discussion towards the first ( $\mathcal{N}_1$ ) and second ( $\mathcal{N}_2$ ) normal stress differences, calculated as [19]

$$\mathcal{N}_1 = \frac{p_{xx} - p_{yy}}{p} \quad \text{and} \quad \mathcal{N}_2 = \frac{p_{yy} - p_{zz}}{p}. \quad (3)$$

For a fixed  $\gamma$ , inelasticity amplifies  $\mathcal{N}_1$  (see figure 7(a)), a trend predicted by the Burnett-order theory for the uni-

form shear flow [18, 20]. For a fixed  $e_n$ ,  $\mathcal{N}_1$  increases with increasing  $\gamma$  as expected. Notably  $\mathcal{N}_1$  remains positive for all values of  $e_n$  and  $\gamma$  simulated. For the case of asymmetric thermal walls, i.e.  $\Delta T_w \neq 0$  [12], this shear dependence of  $\mathcal{N}_1$  was predicted both by DSMC and analytical solution based on Grad's method [13]. The latter work also predicted negative  $\mathcal{N}_1$  for very low values of the reduced shear rate  $a$ , although we do not observe  $\mathcal{N}_1 < 0$ .

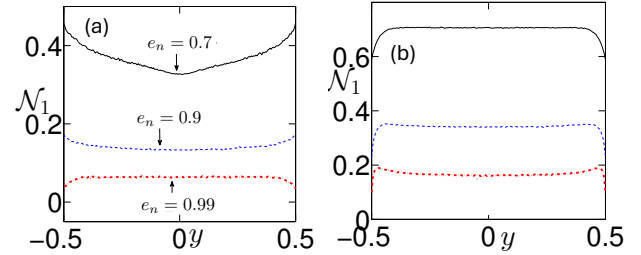


**Figure 7.** Profiles of first normal stress difference ( $\mathcal{N}_1$ ) for  $e_n = 0.7, 0.9, 0.99$ , with  $\gamma =$  (a) 80 and (b) 400.

Inelasticity increases the magnitude of  $\mathcal{N}_2$  (fig. 8a), but the dependence of  $\mathcal{N}_2$  on  $\gamma$  is more nontrivial (fig. 8b). While at  $\gamma = 80$ , the values of  $\mathcal{N}_2$  for  $e_n = 0.9, 0.7$  are both positive (in the bulk), they become negative at  $\gamma = 400$ , indicating that increasing shear rate makes the second normal stress difference negative. A similar sign-change in the second normal-stress difference was found in granular Poiseuille flow [11]. We note that theoretical [18, 20] and simulation [19] works on uniform-shear flow have found  $\mathcal{N}_2 < 0$  in the dilute limit, and  $\mathcal{N}_2$  becomes positive beyond a threshold particle fraction of 10% [18, 19]. We speculate that the local clustering induced by inelasticity ( $e_n = 0.7, 0.9$ ) at low values of  $\gamma$ , increases the centreline particle fraction beyond the threshold for negative  $\mathcal{N}_2$ . This issue requires a detailed analysis to confirm.

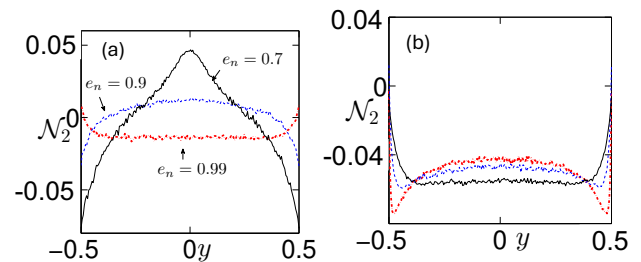


**Figure 8.** Profiles of second normal stress difference ( $\mathcal{N}_2$ ) for  $e_n = 0.7, 0.9, 0.99$ , with  $\gamma =$  (a) 80 and (b) 400.

Finally, we report on the tangential and parallel heat-flux, denoted by  $q_x$  and  $q_y$ , respectively. Note that a non-zero  $q_x$  is a non-Fourier effect since there is no temperature gradient in the flow ( $x$ ) direction. In figure 9, we report heat-fluxes for three different values of  $\gamma$  from across the phase plot in figure 4(a). Interestingly, both the heat fluxes are oppositely signed which means that in regions of positive  $q_x$ ,  $q_y$  is negative and vice versa. Also, these regions of  $+/-$  heat flux 'switch' on increasing shear rate. This switch occurs approximately when the value of  $\gamma$

crosses over the phase boundary denoting  $\pm \rho''(0)$  in figure 4(a). It is likely that the dissipation-induced clustering and shear-driven rarefaction active across the phase boundary is responsible for moderating this switch. In this regard, the generalized Fourier law [21] can help to understand the switch in the heat flux profiles in figure 9, along with the density and temperature profiles in figures 3 and 5.

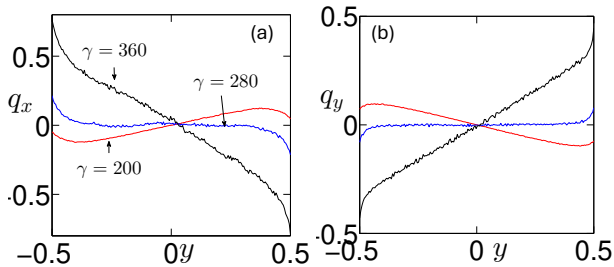


**Figure 9.** (a) Tangential ( $q_x$ ) and (b) wall-normal ( $q_y$ ) heat flux profiles for different  $\gamma$  at  $e_n = 0.7$ .

## 4 Conclusions

We have analysed the plane Couette flow of a dilute granular gas made of smooth inelastic spheres using Direct Simulation Monte Carlo method. We find that the particle clustering induced by inelastic collisions impacts the hydrodynamic and rheological fields. By reframing an increase in shear-rate as a ‘rarefaction’-inducing parameter, we constructed a phase-map (figure 4a) for the sign-change in density curvature at the channel centreline. The competition between inelasticity-induced clustering and shear-induced de-clustering is responsible for the above sign-change. Certain features of higher-order transport coefficients (such as normal stress differences and anisotropic thermal conductivity) are directly tied to the two competing mechanisms operating in different parts of the phase map as well as in different parts of the channel gap, and will be discussed in the conference.

The present simulations are likely to be useful to test nonlinear constitutive relations [18, 20] developed for granular gases, much like the recent work on the Poiseuille flow of a granular gas [21]. It is likely that boundary conditions play a critical role in the dynamics of Couette flow. Testing for different implementations of wall conditions is necessary to equip theoretical models with the ability to make accurate predictions for wall-bounded granular flows.

## References

- [1] C.S. Campbell, Rapid granular flows. *Annu. Rev. Fluid Mech.* **22**, 57 (1990).
- [2] T. Pöschel and S. Luding *Granular Gases*. (Springer, Heidelberg, 2001).
- [3] I. Goldhirsch, Rapid granular flows. *Annu. Rev. Fluid Mech.* **35**, 267 (2003).
- [4] J.T. Jenkins, M.W. Richmann, Kinetic theory of plane flows of a dense gas of identical, rough, inelastic, circular disks. *Phys. Fluids* **28**, 3485-3494 (1985).
- [5] J.J. Brey, J.W. Dufty, C.S. Kim and A. Santos, Hydrodynamics for granular flow at low density. *Phys. Rev. E* **58**, 4638-4653 (1998).
- [6] J.M. Montanero, V. Garzo, M. Alam, and S. Luding, Rheology of two- and three-dimensional granular mixtures under uniform shear flow: Enskog kinetic theory versus molecular dynamics simulations. *Granul. Matt.* **8**, 103-115 (2006).
- [7] V. Garzo, A. Santos and J.M. Montanero, Modified Sonine approximation for the Navier-Stokes transport coefficients of a granular gas. *Physica A* **376**, 94-107 (2007).
- [8] N.V. Brilliantov and T. Pöschel, *Kinetic Theory of Granular Gases*. (Oxford University Press, Oxford, 2004).
- [9] G.A. Bird, *Molecular Gas Dynamics and the Direct Simulation Monte Carlo of Gas Flows*. (Clarendon, Oxford, 1994).
- [10] T. Pöschel and T. Schwager, *Computational Granular Dynamics* (Springer, 2005).
- [11] R. Gupta and M. Alam, Disentangling the role of athermal walls on the Knudsen paradox in molecular and granular gases. *Phys. Rev. E*, **97**.1, 012912 (2018).
- [12] F.V. Reyes, A. Santos, and V. Garzó, Steady base states for non-Newtonian granular hydrodynamics. *J. Fluid Mech* **719**, 431 (2013).
- [13] H. Grad. On the kinetic theory of rarefied gases. *Commun. Pure Appl. Maths.* **2**, 331-407 (1949).
- [14] C. Chapman and T.G. Cowling, *Mathematical Theory of Non-Uniform Gases*. Cambridge University Press (1970)
- [15] R. Gupta and M. Alam, Hydrodynamics, wall-slip, and normal-stress differences in rarefied granular Poiseuille flow. *Phys. Rev. E*, **95**(2), 022903 (2017).
- [16] R. Gupta, DSMC Simulations of Rarefied Granular Gases : Hydrodynamics, Rheology and Segregation (M.S. Thesis), JNCASR, Bangalore (2017)
- [17] M. Tij, E. E. Tahiri, J. M. Montanero, V. Garzó, A. Santos, J. W. Dufty, Nonlinear Couette flow in a low density granular gas. *J. Stat.Phys.* **103**, 1035-1068 (2001).
- [18] S. Saha and M. Alam, Normal stress differences, their origin and constitutive relations for a sheared granular fluid. *J. Fluid Mech.* **795**, 549-580 (2016).
- [19] M. Alam and S. Luding, Non-Newtonian granular fluid: simulation and theory. In *Powders and Grains* (Eds. R. Garcia-Rojo, H.J. Herrmann and S. McNamara), pp. 1141-1145, Balkema (2005).
- [20] N. Sela, and I. Goldhirsch, Hydrodynamic equations for rapid flows of smooth inelastic spheres, to Burnett order. *J. Fluid Mech.* **361**, 41-74 (1998)
- [21] M. Alam, R. Gupta, and S. Ravichandir, Shear-induced heat transport and the relevance of generalized Fourier’s law in granular Poiseuille flow. *Phys. Rev. Fluids*, **6**.11, 114303 (2021)